Chemical Science

EDGE ARTICLE

View Article Online
View Journal | View Issue

Cite this: *Chem. Sci.*, 2019, **10**, 6868

Formation of an imidazoliumyl-substituted $[(L_C)_4P_4]^{4+}$ tetracation and transition metal mediated fragmentation and insertion reaction (L_C = NHC)†

Kai Schwedtmann,[a] Jan Haberstroh,‡[a] Sven Roediger,‡[a] Antonio Bauzá,[b] Antonio Frontera,[b] Felix Hennersdorf[a] and Jan J. Weigand*[a]

Received 7th April 2019
Accepted 29th May 2019

DOI: 10.1039/c9sc01701a

rsc.li/chemical-science

Tetracationic cyclo-tetraphosphane $[(L_C)_4P_4]^{4+}$ as triflate salt (**3**[OTf]$_4$) (L_C = 4,5-dimethyl-1,3-diisopropyl-imidazol-2-yl) is obtained in high yield from the reduction of $[L_CPCl_2]^+$ (**4**[OTf]) with 1,4-bis(trimethylsilyl)-1,4-dihydropyrazine (**6**) and represents the first salt of the cationic cyclo-phosphane series with the general formula $[L_nP_n]^{n+}$. Theoretical calculations reveal the electrophilic nature of the P atoms within the P_4-ring due to the influence of the imidazoliumyl-substituents. Further reduction of **3**[OTf]$_4$ with **6** affords the unexpected formation of the notricyclane P_7-type cation $[(L_C)_3P_7]^{3+}$ (**9**[OTf]$_3$). Selective transition metal mediated [2 + 2]-fragmentation of $\mathbf{3}^{4+}$ is achieved when **3**[OTf]$_4$ is reacted with $Fe_2(CO)_9$, $Pd(PPh_3)_4$ and $Pt(PPh_3)_4$ leading to the formation of the dicationic diphosphene complexes $[(\eta^2\text{-}L_CP{=}PL_C)Fe(CO)_4]^{2+}$ (**12**[OTf]$_2$) and $[(\eta^2\text{-}L_CP{=}PL_C)M(PPh_3)_2]^{2+}$ (**13**[OTf]$_2$ for M = Pd; **14**[OTf]$_2$ for M = Pt). In contrast, the reaction of **3**[OTf]$_4$ with an excess of AuCl(tht) gives rise to the formation of the five-membered ring complex $[((L_C)_4P_4)AuCl_2]^{3+}$ (**15**[OTf]$_3$), where the Au(I) atom reductively inserts into a P–P bond of $\mathbf{3}^{4+}$.

Introduction

The fact that phosphorus tends to assemble into homo-nuclear cyclic and cage-like structural motifs is not only illustrated by the variety of phosphorus allotropes,[1] but also by the multitude of known polyphosphanes.[2] Particularly, neutral monocyclic polyphosphanes with the general formula P_nR_n (R = alkyl, aryl, $n = 3$–5) are already known for decades and their chemistry is well established.[3–5] There are several synthetic protocols for this group of compounds, of which the reduction of a dichlorophosphane $RPCl_2$ (R = alkyl, aryl) with various reducing agents represents the most common approach.[6] The steric demand of the substituents at the P atom determines the favored ring-size.[6,7] Thus, the reduction of $CyPCl_2$ with Mg yields the thermodynamically favored cyclo-Cy_4P_4,[8] whereas the reduction of $PhPCl_2$ gives mainly cyclo-Ph_5P_5.[9] A mixture of compounds with several ring sizes is often observed in the initial reaction, however, a scrambling to the thermodynamically favored ring-size typically occurs over time.[6–9] When the steric demand of the substituent is too large, the formation of cyclo-phosphanes does not proceed, as illustrated by the reduction of Mes*PCl_2 (Mes* = 2,4,6-tri(*tert*-butyl)phenyl) to diphosphene Mes*–P=P–Mes*.[10] Generally, mixed-substituted or cationic cyclo-phosphanes are very scarce and the only examples of dicationic cyclo-phosphanes of type $[R_2(L_C)_2P_4]^{2+}$ ($\mathbf{2a,b}^{2+}$) (L_C = 1,3-bis(2,6-diisopropylphenyl)-imidazol-2-yl, **1a:** R = Ph, **1b:** R = NMe_2; Scheme 1) were recently introduced by Grützmacher and co-workers as a result of a GaCl$_3$-induced

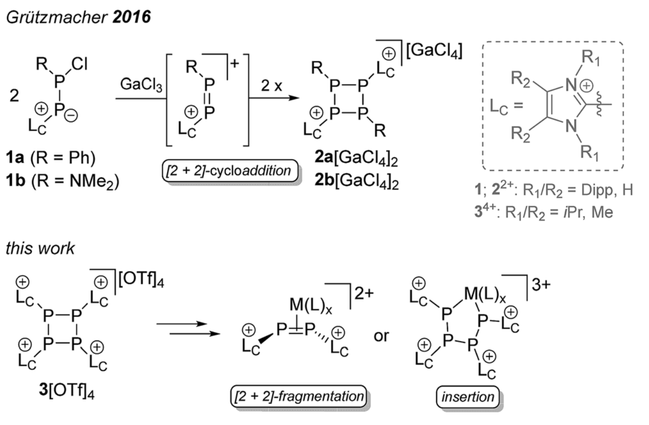

Scheme 1 Cationic cyclo-phosphanes of type $[R_2(L_C)_2P_4]^{2+}$ ($\mathbf{2a,b}^{2+}$) and $[(L_C)_4P_4]^{4+}$ ($\mathbf{3}^{4+}$) and subsequent transition metal mediated fragmentation and insertion reactions.

---

[a] Faculty of Chemistry and Food Chemistry, TU Dresden, Chair of Inorganic Molecular Chemistry, 01062 Dresden, Germany. E-mail: jan.weigand@tu-dresden.de

[b] Department of Chemistry, Universitat de Illes Balears, 07122 Palma de Mallorca, Spain

† Electronic supplementary information (ESI) available. CCDC 1884156–1884162 and 1904570. For ESI and crystallographic data in CIF or other electronic format see DOI: 10.1039/c9sc01701a

‡ These authors contributed equally to this work.

dimerization reaction of **1a,b**.[11] Mechanistically, it has been shown that cyclo-phosphanes **2a,b**$^{2+}$ are formed *via* a [2 + 2]-cycloaddition of the generated diphosphene intermediates. We targeted the replacement of all substituents R in cyclo-P_nR_n by an imidazoliumyl-substituent L_C, resulting in the new group of cationic cyclo-phosphanes of type $[(L_C)_nP_n]^{n+}$ (Scheme 1). These cationic substituents L_C are frequently employed in phosphorus chemistry as they are known to have a significant influence on the reactivity of the directly bonded P atom.[12–15] In this contribution we present the formation of a tetracationic cyclo-tetraphosphane $[(L_C)_4P_4]^{4+}$ as triflate salt (**3**[OTf]$_4$) *via* the reduction of $[L_CPCl_2]^+$ (**4**[OTf])[12] and elucidate the mechanism for its formation. Furthermore, the reductive build-up reaction to a larger cationic phosphorus framework and selective transition metal mediated [2 + 2]-fragmentation and ring opening reactions were investigated.

Results and discussion

We first reduced compound **4**[OTf] with Mg in THF and observed the formation of a yellow-colored reaction mixture (Scheme 2). After removing $MgCl_2$ by filtration, the ^{31}P NMR spectrum of the obtained clear solution reveals a singlet resonance at $\delta(P) = -24.0$ ppm. This resonance can be attributed to the chloride bridged P_2-compound **5**[OTf] which was confirmed by X-ray analysis (see Fig. S2†).[16] As compound **5**[OTf] is similar to our previous findings, in which we employed a sterically more demanding imidazoliumyl-substituent (L_C = 1,3-bis(2,6-diisopropylphenyl)-imidazol-2-yl), we abstain from a detailed discussion here.[17,18] It is noteworthy to mention, however, that reduction of **4**[OTf] with Na gives the same result. The reduction proceeds completely different when **4**[OTf] is reacted with 1,4-bis(trimethylsilyl)-1,4-dihydropyrazine (**6**) in fluorobenzene as solvent. Within 12 h the formation of a colorless precipitate is observed which after filtration and removal of all volatiles *in vacuo* gives the analytically pure triflate salt of the tetracationic cyclo-tetraphosphane **3**$^{4+}$ in very good yield (86%, Scheme 2). Although compound **3**[OTf]$_4$ is well soluble in CH_3CN it slightly decomposes in solution in the course of several days. The ^{31}P NMR spectrum of **3**[OTf]$_4$ dissolved in CD_3CN, shows a singlet resonance at $\delta(P) = -55.7$ ppm, which is comparable to $^tBu_4P_4$ ($\delta(P) = -58.1$ ppm).[19] Single crystals suitable for X-ray analysis are obtained by slow diffusion of Et_2O into a saturated CH_3CN solution of **3**[OTf]$_4$ at −35 °C. Fig. 1 shows the molecular structure of tetracation **3**$^{4+}$ and reveals the typical butterfly-shaped P_4 motif with an averaged P–P–P angle of 81.59°. All imidazoliumyl-substituents at the P_4 ring system are arranged in equatorial and all-*trans* position. The P–P bond lengths in **3**$^{4+}$ (av. 2.235 Å) are in the range for P–P single bonds (2.22 Å)[20] and the P–C bond lengths (av. 1.822 Å) are similar to comparable imidazoliumyl-substituted phosphorus compounds.[15] In order to elucidate whether the formation of tetracation **3**$^{4+}$ proceeds through a diphosphene intermediate, we monitored the aforementioned reaction by means of ^{31}P NMR spectroscopy (see Fig. S3†). Notably, Tamm and co-workers recently reported on the isolation of a diphosphene derivative obtained by the reduction of related dichlorophosphane with compound **6**.[21] The ^{31}P NMR spectrum of the reaction mixture shows only one major prominent intermediate with a singlet resonance at $\delta(P) = -29.1$ ppm, which is in the range for diphosphanes.[22] We assign this intermediate to dication **7**$^{2+}$ which is similar to findings of Goicoechea and co-workers who isolated a related dibromo-diphosphane compound featuring imidazoliumyl-substituents.[18] To further proof our assumption we calculated the chemical shift of intermediate **7**$^{2+}$ and found a theoretical ^{31}P NMR shift of $\delta(P) = -33.4$ ppm being in a reasonable range compared to the experimentally found shift.[16,23] We confirmed the existence of dication **7**$^{2+}$ by the addition of a chloride source, namely $nBu_4N[Cl]$ and observed the formation of chloride-bridged cation **5**$^+$ from **7**$^{2+}$.[16]

Mechanistically, we propose that 2 equivalents of **4**$^+$ react with one equivalent of **6** to give intermediate **7**$^{2+}$ which subsequently reacts with another equivalent of **6** ultimately leading to tetracation **3**$^{4+}$. The first reduction step might also lead to the formation of an $[L_CP]^+$-synthon which is supported by the formation of $[(L_C)_3P_3]^+$ (**8**$^{3+}$) in this reaction (Scheme 3). A few

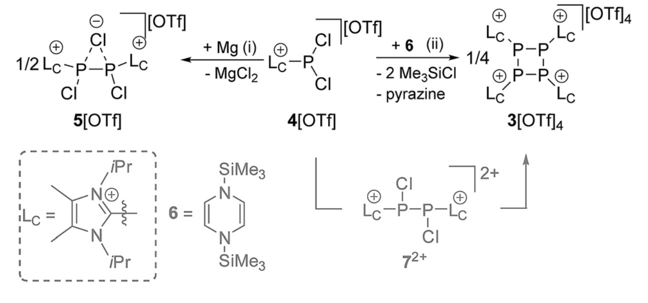

Scheme 2 Reduction of **4**[OTf] with Mg (left) and **6** (right) yields either **5**[OTf] or **3**[OTf]$_4$, respectively. Proposed reaction pathway with intermediate **7**$^{2+}$ to **3**[OTf]$_4$ (grey); (i): +ex. Mg, 12 h, $-2MgCl_2$, 99% (determined by ^{31}P NMR spectroscopy); (ii): +**6**, C_6H_5F, 12 h, −pyrazine, $-2Me_3SiCl$, 86%.

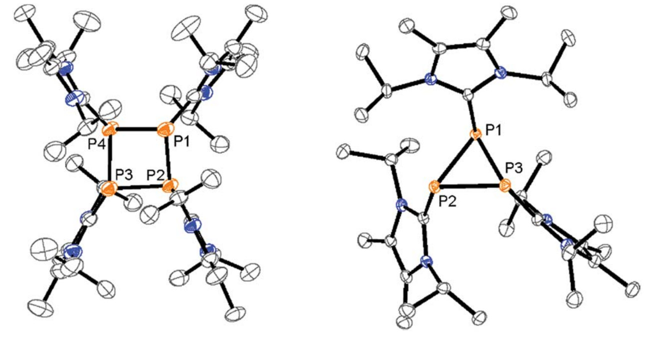

Fig. 1 Molecular structures of tetracation **3**$^{4+}$ in **3**[OTf]$_4$·$2CH_3CN$ (left) and trication **8**$^{3+}$ in **8**[OTf]$_3$ (right; hydrogen atoms, solvate molecules and anions are omitted for clarity and thermal ellipsoids are displayed at 50% probability); selected bond lengths (Å) and angles (°) for **3**$^{4+}$: P1–P2 2.2382(8), P2–P3 2.2356(8), P3–P4 2.2400(8), P4–P1 2.2298(8), P1–C1 1.822(2), P2–C12 1.824(2), P3–C23 1.823(2), P4–C34 1.822(2); P4–P1–P2 81.69(3), P1–P2–P3 81.54(3), P2–P3–P4 81.53(3), P3–P4–P1 81.62(3); **8**$^{3+}$: P1–P2 2.2459(6), P2–P3 2.2293(6), P1–P3 2.2139(6), P1–C1 1.8429(17), P2–C12 1.8373(17), P3–C23 1.8303(17); P1–P2–P3 59.300(18); P2–P3–P1 60.72(2), P3–P1–P2 59.975(18).

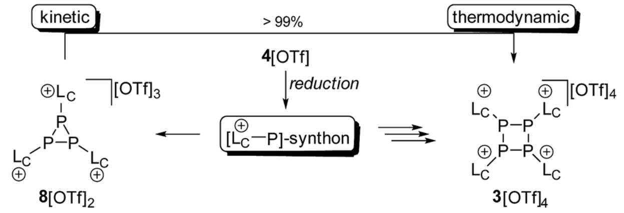

Scheme 3 Formation of 3[OTf]$_4$ and 8[OTf]$_3$ from the proposed [L$_C$–P]$^+$-synthon by reduction of 4[OTf]. Compound 8[OTf]$_3$ readily rearranges in a CH_3CN solution at room temperature within 24 h to 3[OTf]$_4$.

crystals of **8**[OTf]$_3$ could be isolated by overlaying the filtrate of the aforementioned reaction with *n*-hexane at −35 °C. The molecular structure is depicted in Fig. 1. The bonding parameters of trication **8**$^{3+}$ are well in the expected range. Accordingly, one imidazoliumyl-substituent at the planar P_3 ring is *trans*-arranged to the other two imidazoliumyl-substituents which results in the characteristic pattern in the ^{31}P NMR spectrum.[3,6] The ^{31}P NMR spectrum of **8**$^{3+}$ shows the AB$_2$ spin system ($\delta(P_A) = -142.5$ ppm, $\delta(P_B) = -130.8$ ppm; $^1J(PP) = -162$ Hz) in the typical region for cyclo-triphosphanes.[19] To our surprise, time dependent ^{31}P NMR spectra reveal the rearrangement of **8**$^{3+}$ into cyclo-tetraphosphane **3**$^{4+}$ in a CD_3CN solution in the course of 24 h (Fig. 2), suggesting that **8**$^{3+}$ is the kinetic product of this reaction, while **3**$^{4+}$ is thermodynamically favorable. Although such ring expansions are known for neutral cyclo-phosphanes, it seems, due to electrostatic repulsive effects, thermodynamically contradicting that a trication (**8**$^{3+}$) transforms into the corresponding tetracation (**3**$^{4+}$),[24] rather than its fragmentation into charge separated species.[24,25] We calculated the HOMO and the LUMO and optimized the structure by DFT methods using the PBE0/def2-TZVP level of theory (Fig. 3).[16] The HOMO of cation **3**$^{4+}$ is basically located at the imidazoliumyl-substituents, whereas the LUMO is mostly located at the P_4 ring, suggesting an electrophilic nature of the P atoms within the P_4 ring. The small degree of delocalization of the LUMO onto the imidazoliumyl-substituents also contributes to the stability of the tetracation **3**$^{4+}$. We further reduced cyclo-tetraphosphane **3**[OTf]$_4$ again using the metal free reducing agent **6** (Scheme 4). Upon reaction of **3**[OTf]$_4$ with **6** in CH_3CN, the reaction mixture turned from colorless to orange. The ^{31}P NMR spectrum of this mixture showed after 8 hours a broad singlet resonance at $\delta(P) = -124.6$ ppm and a dynamic AA′A″BXX′X″ spin system with resonances at $\delta(P_A) = -178.5$ ppm, $\delta(P_B) = -164.9$ ppm and $\delta(P_X) = 13.2$ ppm (see Fig. S5†).[16] The singlet resonance is assigned to cation **10**$^+$ which was first reported by Macdonald and co-workers[26] whereas the spin system of higher order is attributed to the P_7 trication $[(L_C)_3P_7]^{3+}$ (**9**$^{3+}$). Imidazolium cation **11**$^+$ has been identified by its characteristic chemical shift in the ^{29}Si NMR spectrum.[12] **9**[OTf]$_3$ can be isolated by washing the obtained crude oil with THF and CH_2Cl_2. After removal of all volatiles *in vacuo*, salt **9**[OTf]$_3$ is obtained as colorless solid in an overall yield of 61%. Fig. 3 shows the ^{31}P{H} NMR spectrum of **9**$^{3+}$ at 260 K which is iteratively fitted to an AA′A″BXX′X″ spin system and indicates the formation of a C_3-symmetric stereoisomer (Fig. 4).[27] The A part at $\delta(P_A) = -178.5$ ppm is assigned to the P atoms of the basal P_3-ring, the B part at $\delta(P_B) = -164.9$ ppm to the apical P atom and the X part at $\delta(P_X) = 13.2$ ppm to the bridging P atoms carrying the imidazoliumyl-substituents. Details on coupling constants are included in the ESI in Table S1.† Single crystals suitable for X-ray analysis are obtained by slow diffusion of CH_2Cl_2 into a saturated CH_3CN solution of **9**[OTf]$_3$ at −35 °C. The molecular structure confirms the C_3-symmetric, heptaphosphanortricyclane cage with three imidazoliumyl-substituents at the bridging phosphorus atoms P2, P3 and P4 (Fig. 4). The P–C bond lengths (av. 1.834 Å) are comparable to those of tetracation **3**$^{4+}$ (av. 1.822 Å) and other imidazoliumyl-substituted

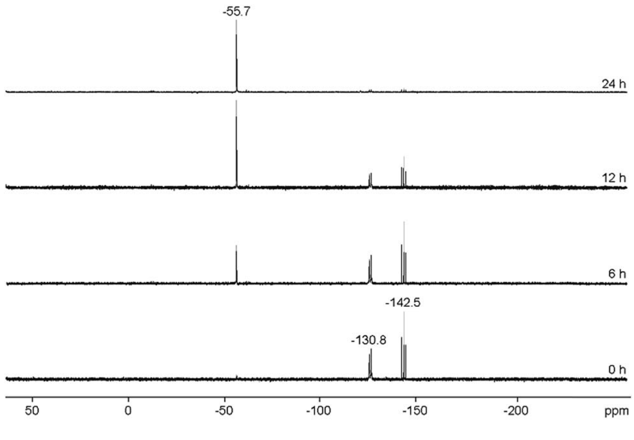

Fig. 2 Time dependent ^{31}P NMR spectra of **8**$^{3+}$, revealing a slow conversion of triphosphirane **8**$^{3+}$ into cyclo-tetraphosphane **3**$^{4+}$ over the course of 24 h (300 K, CD_3CN). The resonances can be assigned as follows: $\delta(P) = -55.7$ ppm to **3**$^{4+}$; and AB$_2$ spin system $\delta(P_A) = -142.5$ ppm, $\delta(P_B) = -130.8$ ppm to **8**$^{3+}$.

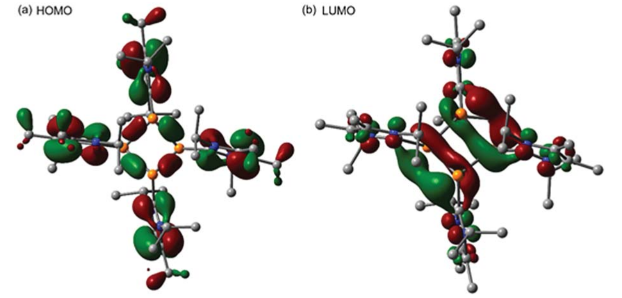

Fig. 3 HOMO (a) and LUMO (b) from the DFT optimized structure of **3**$^{4+}$ using the PBE0/def2-TZVP functional.

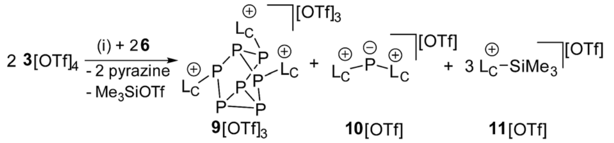

Scheme 4 Reaction of **3**[OTf]$_4$ with **6** to **9**[OTf]$_3$, **10**[OTf] and **11**[OTf]; (i) +2 **6**, CH_3CN, 8 h, −2 pyrazine, −Me_3SiOTf, 61%.

phosphorus derivatives.[15] The bonding parameters within the P_7-cage are comparable to those of our previously reported triarsonium-substituted P_7 cage compound,[27a] *i.e.* the P–P bond lengths of the basal P atoms and the bridging P atoms (P2–P5, P3–P6 and P4–P7: av. 2.2238 Å) are slightly longer compared to those in the basal P_3-ring (av. 2.2166 Å) and to those between the apical and the bridging P atoms (P1–P2, P1–P3 and P1–P4: av. 2.1882 Å).

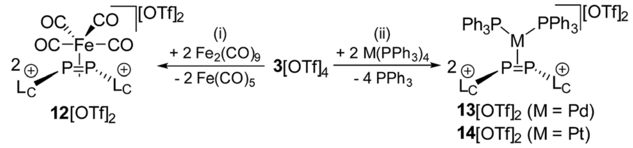

Scheme 5 Transition metal induced [2 + 2]-fragmentation of **3**[OTf]$_4$ to give diphosphene complexes **12**[OTf]$_2$, **13**[OTf]$_2$ and **14**[OTf]$_2$; (i) +2 $Fe_2(CO)_9$, CH_3CN/THF, 12 h, −2 $Fe(CO)_5$, 98%; (ii) +2 $M(PPh_3)_4$ (M = Pd, Pt), CH_3CN/THF, 12 h, −4PPh_3, 93% for **13**[OTf]$_2$ and 88% for **14**[OTf]$_2$.

As the DFT calculations suggest rather electrophilic P atoms in $\mathbf{3}^{4+}$, we investigated its reactivity towards a series of low valent transition metal compounds in order to evaluate the ligand properties of $\mathbf{3}^{4+}$. **3**[OTf]$_4$ readily reacts with two equivalents of $Fe_2(CO)_9$ in a 1 : 1 mixture of THF/CH_3CN under the immediate formation of a brown-colored reaction mixture. The addition of Et_2O gives a yellow-colored precipitate in a 98% yield which was identified as complex **12**[OTf]$_2$.[16] In this complex, a $Fe(CO)_4$ moiety is η^2-coordinated by the disphosphene ligand $[L_CP{=}PL_C]^{2+}$, which is formed *via* the metal induced [2 + 2]-fragmentation (Scheme 5). Single crystals suitable for X-ray analysis are obtained by slow diffusion of *n*-hexane into a saturated CH_2Cl_2 solution of **12**[OTf]$_2$. The complex reveals a trigonal core including the P atoms of the $[L_CP{=}PL_C]^{2+}$ ligand and the Fe atom of the $Fe(CO)_4$ moiety. The imidazoliumyl-substituents of the $[L_CP{=}PL_C]^{2+}$ ligand are arranged in an *E*-configuration (C1–P1–P2–C12 149.205(1)°) and the P1–Fe–P2 angle is relatively acute with a value of 54.490(19)°. The shortest distance between the diphosphene unit and the Fe atom is 2.105 Å as a result of the rather long Fe–P contacts (Fe–P1 2.3774(6) Å and Fe–P2 2.3590(6) Å). In contrast, typically Fe–P distances in η^1-coordination complexes are usually in the region of 2.2 Å.[28] The P–P bond length with a value of 2.1684(7) Å is significantly longer compared to those in a typical diphosphene such as Mes*–P=P–Mes*: (2.034(2) Å),[10] but slightly shorter compared to a typical P–P single bond (compare $\mathbf{3}^{4+}$: av. 2.235 Å). This also supports the η^2-coordination of the P_2 ligand. The IR stretching frequencies of the CO ligands are found at 2048 cm^{-1}, 2074 cm^{-1} and 2116 cm^{-1} and are significantly shifted to higher wave numbers compared to related reported phosphorus $Fe(CO)_4$ complexes (*e.g.* $[(L_2{-}P{-}L_2)Fe(CO)_4][BPh_4]$: 2029 cm^{-1}, 1947 cm^{-1}, 1907 cm^{-1}).[29] According to Tolman analysis,[30] this suggests that the $[L_CP{=}PL_C]^{2+}$ ligand is a very strong π-acceptor which even surpasses PF_3 ($[(PF_3)Fe(CO)_4]$: 2101 cm^{-1}, 2022 cm^{-1}, 2018 cm^{-1}, 1999 cm^{-1})[31] due to the electron withdrawing effect of the imidazoliumyl-substituents.[16,32] We therefore computed the π-accepting properties of the $[L_CP{=}PL_C]^{2+}$ ligand which is related to the LUMO energy and shape of the ligand (see Fig. S12†).[16] Our calculations show that the LUMO is the π*(P=P) bond which is perfectly pre-organized to interact with the d-orbitals of the Fe atom. Furthermore, the calculations indicated that, due to the dicationic charge, the LUMO is very low in energy (−9.313 eV; compare $[L_C{-}P{=}P{-}Dipp]^+$: −5.900 eV;[16,33] L_C = 4,5-dichloro-1,3-bis(Dipp)-imidazol-2-yl; Dipp = 2,6-diisopropylphenyl; see Fig. S12†) which is beneficial for π-bonding with the corresponding transition metal. In addition, the second order perturbation analysis of $\mathbf{12}^+$ reveals a strong back-bonding from the d-orbitals of the Fe atom into the σ*(P–C)-orbital ($E^{(2)}$ = 35.77 kcal mol^{-1}) indicating the stability of this complex.[16] Similar findings have been recently reported by Macdonald and

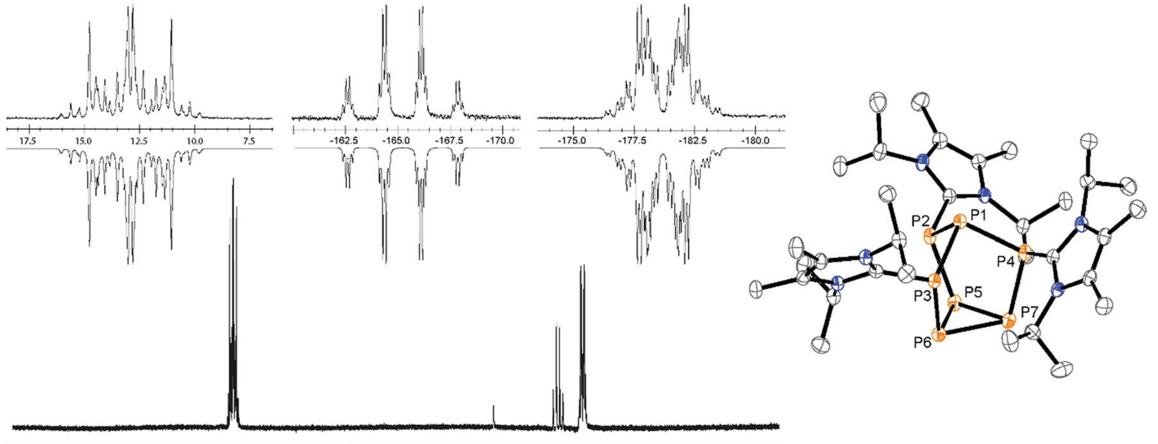

Fig. 4 $^{31}P\{H\}$ NMR spectrum of $\mathbf{9}^{3+}$ (CD_3CN, 260 K). Insets show the extension of the experimental (upwards) and the iteratively fitted (downwards) AA′A″BXX′X″ spin system (left); molecular structure of trication $\mathbf{9}^{3+}$ in **9**[OTf]$_3\cdot 0.8CH_3CN\cdot 1.7CH_2Cl_2$ (right); hydrogen atoms, solvate molecules and anions are omitted for clarity and thermal ellipsoids are displayed at 50% probability; selected bond lengths (Å) and angles (°) for: P1–P2 2.1810(6), P1–P3 2.1816(6), P1–P4 2.2022(6), P2–P5 2.2189(7), P3–P6 2.2282(7), P4–P7 2.2243(7), P5–P6 2.2250(7), P5–P7 2.2021(7), P6–P7 2.2227(7), P2–C1 1.8339(19), P3–C12 1.8291(19), P4–C23 1.8418(19).

co-workers for a related diphosphene nickel complex featuring two phosphoniumyl-substituents.[34]

Similar [2 + 2]-fragmentation reactions are observed when **3**[OTf]$_4$ is reacted with 2 equivalents of M(PPh$_3$)$_4$ (M = Pd, Pt) in a 1 : 1 mixture of THF/CH$_3$CN which leads to the formation of diphosphene complexes **13**[OTf]$_2$ (Pd(PPh$_3$)$_4$) and **14**[OTf]$_2$ (Pt(PPh$_3$)$_4$), respectively, under concomitant release of 4 equivalents PPh$_3$ (Scheme 5). After workup, complexes **13**[OTf]$_2$ and **14**[OTf]$_2$ are obtained as analytically pure red-colored (**13**[OTf]$_2$, 93%) or yellow-colored (**14**[OTf]$_2$, 88%) crystalline powders. The ^{31}P NMR spectrum of **13**[OTf]$_2$ at 300 K shows a broad singlet resonance at $\delta(P) = 10.2$ ppm for the phosphorus atoms of the diphosphene moiety which upon cooling to 270 K appears as *pseudo* triplet with a $^2J(PP)$ coupling constant of 31 Hz. The two PPh$_3$ ligands give rise to a *pseudo*-triplet resonance at $\delta(P) = 23.4$ ppm ($^2J(PP) = 31$ Hz). The chemical shift is comparable to the related diphosphene complex [(η^2-F$_3$C–P=P–CF$_3$)Pd(PPh$_3$)$_2$].[35] In contrast to the *trans*-$^2J(PP)$ coupling, the magnitude of the *cis* $^2J(PP)$ coupling is not resolved, resulting in the observed *pseudo*-triplet splitting of this resonance. The ^{31}P NMR spectrum of **14**[OTf]$_2$ shows dynamic behavior at 300 K which upon cooling resolves to an AA′BB′X spin system. The high field shifted A part at $\delta(P_A) = -42.9$ ppm is assigned to the diphosphene moiety and shows a $^2J(PP)$ coupling constant of 29 Hz similar to that of **13**[OTf]$_2$. The $^1J(PPt)$ coupling with a value of 235 Hz is significantly smaller compared to typical $^1J(PPt)$ coupling constants,[35] indicating the η^2-coordination of the disphosphene ligand and the Pt atom.[35,36] The B part at $\delta(P_B) = 25.1$ ppm ($^2J(PP) = 29$ Hz) is assigned to the PPh$_3$ ligands and reveals a typical $^1J(PPt)$ coupling constant of 3279 Hz. The ^{195}Pt NMR spectrum shows a triplet of triplet resonance at $\delta(Pt) = -5015.7$ ppm ($^1J(PtP) = 3279$ Hz; $^1J(PtP) = 235$ Hz; see Fig. S8†). For both complexes a set of resonances with low intensities indicates the presence of rotational isomers in the NMR spectra which, however, only appears at temperatures below 270 K (see Fig. S6 and S7†). Single crystals suitable for X-ray analysis are obtained for both complexes by slow diffusion of Et$_2$O into a saturated CH$_3$CN solutions (Fig. 5). Similar to complex **12**[OTf]$_2$, the η^2-coordination of the corresponding metal by the diphosphene ligand is observed with the metal atoms being in a distorted square planar bonding environment. The averaged distance between the diphosphene unit and metals are in the same range (**13**$^{2+}$: Pd⋯P–P 2.124 Å, Pd–P1 2.3543(6) Å, Pd–P2 2.4003(8) Å; **14**$^{2+}$: Pt⋯P–P 2.114 Å, Pt–P1 2.3530(7) Å, Pt–P2 2.3930(6) Å). The P–P bond lengths are only marginally shorter (**13**$^{2+}$ 2.1340(12) Å and **14**$^{2+}$ 2.1562(9) Å) compared to that of complex **12**$^{2+}$ (2.1684(7) Å). Similar to the Fe complex the [L$_C$P=PL$_C$]$^{2+}$ ligand is in both cases also in the *E*-configuration (**13**$^{2+}$: C1–P1–P2–C12 148.393°; **14**$^{2+}$: C1–P1–P2–C12 147.088°).

Notably, the known diphosphene complexes [(η^2-F$_3$C–P=P–CF$_3$)M(PPh$_3$)$_2$] (M = Pd, Pt)[35,37] are also synthesized from the reaction of the tetraphosphetane (CF$_3$)$_4$P$_4$ and the corresponding transition metal precursor M(PPh$_3$)$_4$ (M = Pd, Pt) suggesting the necessity of electron withdrawing substituents at the P atoms for the observed [2 + 2]-fragmentation. However, the formation of the dicationic diphosphene complexes (**12**$^{2+}$, **13**$^{2+}$ and **14**$^{2+}$), featuring imidazoliumyl-substituents at the P atom, illustrate the potential use of cyclo-tetraphosphane **3**$^{4+}$ to synthesize a variety of novel cationic transition metal complexes. When **3**[OTf]$_4$ is reacted with one equivalent AuCl(tht) in THF/CH$_3$CN (1 : 1) the formation of a small set of two coupled broad resonances at $\delta(P) = -49.9$ ppm and $\delta(P) = -24.7$ ppm along with a singlet resonance for **1**[OTf] ($\delta(P) = 107.8$ ppm) can be observed in the ^{31}P NMR spectrum of the reaction mixture (see Fig. S9†). A complete consumption of **3**[OTf]$_4$ is achieved with 4 equivalents of AuCl(tht) (see Fig. S10†). Filtration of the reaction mixture after 12 h and recrystallization from THF, complex **15**[OTf]$_3$ can be isolated as a yellow powder. The yield can be increased by further recrystallization steps up to 57%. The ^{31}P NMR spectrum of **15**[OTf]$_3$ dissolved in CD$_2$Cl$_2$ shows at 300 K two broad resonances which resolve to an AA′BB′ spin system at 260 K (Fig. 6). The A part at $\delta(P) = -49.9$ ppm can

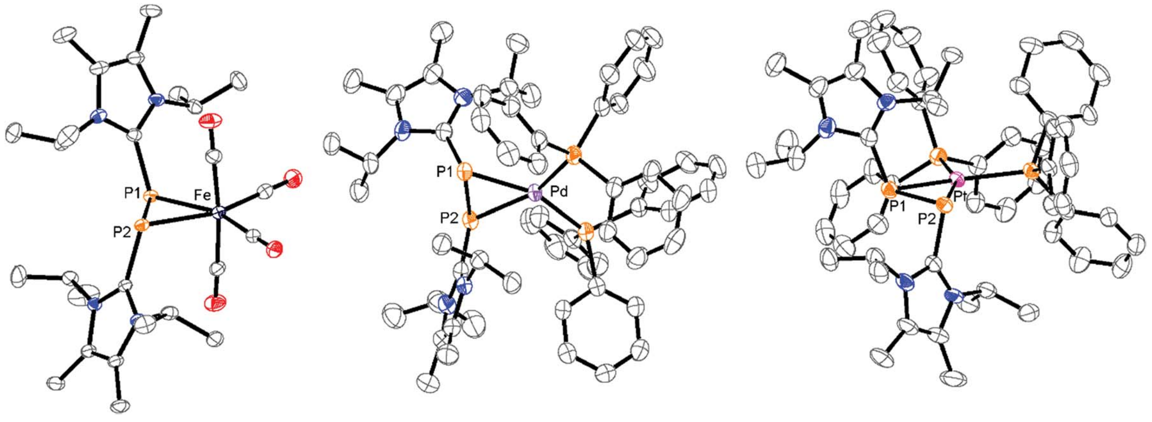

Fig. 5 Molecular structures of diphosphene complexes **12**$^{2+}$ in **12**[OTf]$_2$, **13**$^{2+}$ in **13**[OTf]$_2$·3C$_6$H$_5$F and **14**$^{2+}$ in **14**[OTf]$_2$·3C$_6$H$_5$F; hydrogen atoms, solvate molecules and anions are omitted for clarity and thermal ellipsoids are displayed at 50% probability; selected bond lengths (Å) and angles (°) for **12**$^{2+}$(Fe): P1–P2 2.1684(7), Fe⋯P–P 2.105, Fe–P1 2.3774(6), Fe–P2 2.3590(6); C1–P1–P2–C12 149.205(1), P1–Fe–P2 54.490(19); **13**$^{2+}$(Pd): P1–P2 2.1340(12), Pd⋯P–P 2.124, Pd–P1 2.3543(6), Pd–P2 2.4003(8); C1–P1–P2–C12 148.393; **14**$^{2+}$ (Pt): 2.1562(9), Pt⋯P–P 2.114, Pt–P1 2.3530(7), Pt–P2 2.3930(6); C1–P1–P2–C12 147.088.

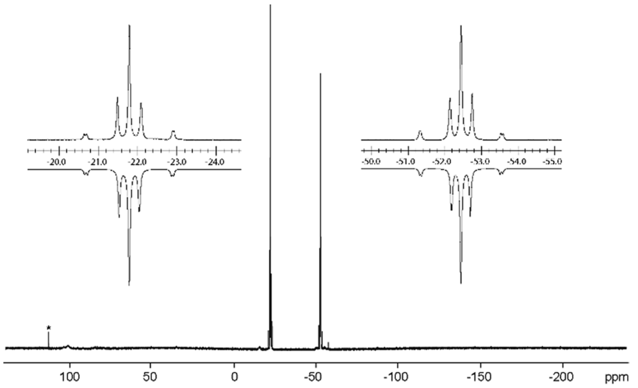

Fig. 6 $^{31}P\{H\}$ NMR spectrum of 15^{3+} (CD_2Cl_2, 260 K). Insets show the extension of the experimental (upwards) and the iteratively fitted (downwards) AA′XX′ spin system; trace amounts of unidentified side product is marked with an asterisk.

be assigned to the backbone P atoms and the B part at $\delta(P) = -24.7$ ppm to the Au-coordinating P atoms. Details on coupling constants are included in the ESI in Table S2.† Single crystals suitable for X-ray analysis are obtained by overlaying a saturated CH_2Cl_2 solution of **15**[OTf]$_3$ with pentane at −35 °C (Fig. 7). The Au atom is coordinated by two P atoms resulting in a five-membered P_4Au-core structure which reveals an envelope conformation. Hey-Hawkins and co-workers reported on a similar structural motif where a *catena*-tetraphophosphane-1,4-diide coordinates Ni(0) and Pd(0), respectively.[38] The gold atom in 15^{3+} reveals a square-planar geometry where the P_4-chain chelates the gold atom *via* P1 and P4. The phosphorus gold bond lengths (P1–Au 2.3053(11) Å and P4–Au 2.3103(10) Å) are well in the range for related P–Au^{III} bonds (av. 2.314).[39] The four P atoms exhibit a pyramidal bonding environment with P–P bond lengths (av. 2.237 Å) being in the range of typical P–P single bonds (2.22 Å).[20] As expected, the bond angles around the phosphorus atoms P1 and P4 (Au–P1–P2 107.79(5) ° and P3–P4–Au 107.90(5) Å) are wider compared to the other angles within the P_4Au-core structure (P1–Au–P4 92.63(4) Å, P1–P2–P3 93.22(5) Å, P2–P3–P4 90.66(5) Å). Different from the above mentioned reactions, the reaction of **3**[OTf]$_4$ with an excess of AuCl leads to a reductive insertion of the gold atom into the P_4-ring of **3**[OTf]$_4$ leading to the formation of a five-membered P_4Au-core structure (Scheme 6).

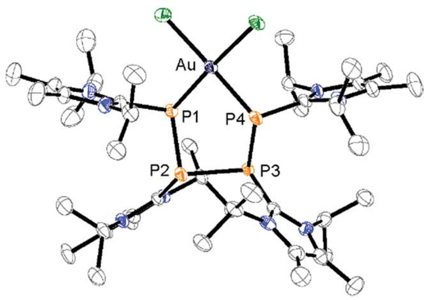

Fig. 7 Molecular structure of gold complex 15^{3+} in **15**[OTf]$_3\cdot 3CH_2Cl_2$; hydrogen atoms, solvate molecules and anions are omitted for clarity and thermal ellipsoids are displayed at 50% probability; selected bond lengths (Å) and angles (°): P1–P2 2.2364(14), P2–P3 2.2304(13), P3–P4 2.2467(15), P1–Au 2.3053(11), P4–Au 2.3103(10); P1–Au–P4 92.63(4), Au–P1–P2 107.79(5), P1–P2–P3 93.22(5), P2–P3–P4 90.66(5), P3–P4–Au 107.90(5).

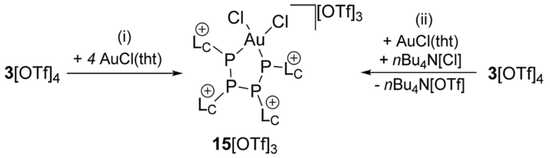

Scheme 6 Formation of the 5-membered P_4Au-complex **15**[OTf]$_3$; (i) +4 AuCl(tht), THF/CH_3CN, 8 h 57%; (ii) +AuCl(tht), +nBu$_4$N[Cl], THF/CH_3CN, −nBu$_4$N[OTf], 76% determined by ^{31}P NMR spectroscopy.

In this reaction, the Au(I) atom reductively inserts into a P–P bond of 3^{4+} and is oxidized to Au(III). The free coordination site at the Au atom is saturated by a further chloride anion, leading to the square planar coordination environment at the Au(III) atom. Thus, it appears that the excess of the AuCl(tht) merely serves as chloride source in this reaction. We found that the reaction can be carried out with one equivalent AuCl(tht) and one equivalent nBu$_4$N[Cl] as chloride source which leads to the consumption of **3**[OTf]$_4$ up to 90% and to the formation of the P_4Au-complex **15**[OTf]$_3$ in 70% yield as judged by ^{31}P NMR spectroscopy (see Fig. S11†).

Conclusions

In summary, we successfully synthesized the first example of a cationic cyclo-phosphane with the general formula $[(L_C)_nP_n]^{n+}$ (**3**[OTf]$_4$) *via* the reduction of **4**[OTf] using 1,4-bis(trimethylsilyl)-1,4-dihydropyrazine (**6**). Due to the electrophilic nature of the P atoms within the P_4 ring, which was shown by theoretical calculations, we further reduced compound **3**[OTf]$_4$ to give the notricyclane P_7 compound **9**[OTf]$_3$. The reaction of **3**[OTf]$_4$ with low oxidation state transition metal complexes $Fe_2(CO_9)$, $Pd(PPh_3)_4$ and $Pt(PPh_3)_4$ leads to the formation of dicationic diphosphene complexes **12**[OTf]$_2$, **13**[OTf]$_2$ and **14**[OTf]$_2$, respectively. The transition metal mediated [2 + 2]-fragmentation reaction of 3^{4+} is attributed to the cationic imidazoliumyl-substituents causing the electrophilic nature of the P atoms in 3^{4+}. Due to the dicationic charge, the P_2 ligand in the aforementioned complexes is a very good π-acceptor with an exceptionally low lying LUMO (π*-P═P bond) rendering this ligand optimal for the complexation of a π-basic metal center. In contrast, the reaction of **3**[OTf]$_4$ with an excess of AuCl(tht) gives rise to the formation of complex **15**[OTf]$_3$ featuring a five-membered P_4Au-core structure. In this reaction, the Au(I) atom reductively inserts into a P–P bond of 3^{4+} and is oxidized to Au(III). As the DFT calculations of the optimized structure of 3^{4+} reveal rather Lewis acidic P atoms, the reactivity towards nucleophiles promises a variety of novel phosphorus compounds featuring interesting bonding motifs and properties.

Conflicts of interest

There are no conflicts to declare.

Acknowledgements

This work was supported by the German Science Foundation (DFG Grant number WE 4621/3-1). A. F. and A. B. thank MINECO/AEI of Spain (project CTQ2017-85821-R FEDER funds) for financial support. We also thank Philipp Lange for experimental assistance and EA measurements.

Notes and references

1 (*a*) D. E. C. Corbridge, *Phosphorus Chemistry, Biochemistry and Technology*, Elsevier, Amsterdam, 2000; (*b*) N. Wiberg, *Lehrbuch der Anorganischen Chemie*, de Gruyter, Berlin, 102 edn, 2007, pp. 758–775.

2 (*a*) A. H. Cowley, *Chem. Rev.*, 1965, **65**, 617; (*b*) L. Lamandé, K. Dillon and R. Wolf, *Phosphorus, Sulfur Silicon Relat. Elem.*, 1995, **103**, 1; (*c*) M. Donath, F. Hennersdorf and J. J. Weigand, *Chem. Soc. Rev.*, 2016, **45**, 1145.

3 Selected examples for the chemistry of neutral triphosphiranes: (*a*) M. Bentner and W. Uhl, *Dalton Trans.*, 2000, 3133; (*b*) C. A. Dyker, N. Burford, G. Menard, M. D. Lumsden and A. Decken, *Inorg. Chem.*, 2007, **46**, 4277; (*c*) M. H. Holtausen, D. Knackstedt, N. Burford and J. J. Weigand, *Aust. J. Chem.*, 2013, **66**, 1155; (*d*) A. P. M. Robertson, C. A. Dyker, P. Gray, B. O. Patrick, A. Decken and N. Burford, *J. Am. Chem. Soc.*, 2014, **136**, 14941; (*e*) S. S. Chitnis, H. A. Sparkes, V. T. Annibale, N. E. Pridmore, E. Natalie, A. M. Oliver and I. Manners, *Angew. Chem., Int. Ed.*, 2017, **56**, 9536; *Angew. Chem.*, 2017, **129**, 9664.

4 Selected examples for the chemistry of neutral tetraphosphetanes: (*a*) S. Parveen, P. Kilian, A. M. Z. Slawin and J. D. Woollins, *Dalton Trans.*, 2006, 2586; (*b*) C. A. Dyker, S. D. Riegel, N. Burford, M. D. Lumsden and A. Decken, *J. Am. Chem. Soc.*, 2007, **129**, 7464; (*c*) J. J. Weigand, N. Burford, R. J. Davidson, T. S. Cameron and P. Seelheim, *J. Am. Chem. Soc.*, 2009, **131**, 17953; (*d*) E. Conrad, N. Burford, U. Werner-Zwanziger, R. McDonald and M. J. Ferguson, *Chem. Commun.*, 2010, **46**, 2465.

5 Selected examples for the chemistry of neutral pentaphospholanes: (*a*) A. J. Arduengo III, H. V. R. Dias and J. C. Calabrese, *Chem. Lett.*, 1997, 143; (*b*) I. P. Gray, P. Bhattacharyya, A. M. Z. Slawin and J. D. Woollins, *Chem.–Eur. J.*, 2005, **11**, 6221; (*c*) R. B. Baker, C. Jones, D. P. Mills, D. M. Murphy, E. Hey-Hawkins and R. Wolf, *Dalton Trans.*, 2006, 64; (*d*) R. Wolf, M. Finger, C. Limburg, C. A. Willis, S. B. Wild and E. Hey-Hawkins, *Dalton Trans.*, 2006, 831; (*e*) S. Geier and D. W. Stephan, *Chem. Commun.*, 2010, **46**, 1026; (*f*) J. H. Barnard, P. A. Brown, K. L. Shuford and C. D. Martin, *Angew. Chem., Int. Ed.*, 2015, **54**, 12083; *Angew. Chem.*, 2015, **127**, 12251.

6 For reviews see: (*a*) M. Baudler and K. Glinka, *Chem. Rev.*, 1993, **93**, 1623; (*b*) G. He, O. Shynkaruk, M. W. Lui and E. Rivard, *Chem. Rev.*, 2014, **114**, 7815.

7 (*a*) L. Weber, *Chem. Rev.*, 1992, **92**, 1839; (*b*) A.-M. Caminade, J.-P. Majoral and R. Mathieu, *Chem. Rev.*, 1991, **91**, 575.

8 L. R. Smith and J. L. Mills, *J. Am. Chem. Soc.*, 1976, **98**, 3852.

9 (*a*) M. Baudler and K. Hammerstroem, *Z. Naturforsch., B: J. Chem. Sci.*, 1965, **20**, 810; (*b*) A. H. Cowley and R. P. Pinnell, *Inorg. Chem.*, 1966, **5**, 459.

10 M. Yoshifuji, I. Shima, N. Inamoto, K. Hirotsu and T. Higuchi, *J. Am. Chem. Soc.*, 1981, **103**, 4587.

11 A. Beil, R. J. Gilliard Jr and H. Grützmacher, *Dalton Trans.*, 2016, **45**, 2044.

12 (*a*) J. J. Weigand, K.-O. Feldmann and F. D. Henne, *J. Am. Chem. Soc.*, 2010, **132**, 16321; (*b*) F. D. Henne, A. T. Dickschat, F. Hennersdorf, K.-O. Feldmann and J. J. Weigand, *Inorg. Chem.*, 2015, **54**, 6849.

13 F. D. Henne, F. A. Watt, K. Schwedtmann, F. Hennersdorf, M. Kokoschka and J. J. Weigand, *Chem. Commun.*, 2016, **52**, 2023.

14 K. Schwedtmann, M. H. Holthausen, K.-O. Feldmann and J. J. Weigand, *Angew. Chem., Int. Ed.*, 2013, **52**, 14204; *Angew. Chem.*, 2013, **125**, 14454.

15 For reviews see: (*a*) K. Schwedtmann, G. Zanoni and J. J. Weigand, *Chem.–Asian J.*, 2018, **13**, 1388; (*b*) T. Krachko and C. Slootweg, *Eur. J. Inorg. Chem.*, 2018, 2734.

16 For details see ESI.†

17 F. D. Henne, E.-M. Schnoeckelborg, K.-O. Feldmann, J. Grunenberg, R. Wolf and J. J. Weigand, *Organometallics*, 2013, **32**, 6674.

18 For the bromide-bridged analogue see: J. B. Waters, T. A. Everitt, W. K. Myers and J. M. Goicoechea, *Chem. Sci.*, 2016, **4**, 77.

19 M. Baudler, J. Hahn, H. Dietsch and G. Fürstenberg, *Z. Naturforsch., B: J. Chem. Sci.*, 1976, **31**, 1305.

20 (*a*) M. Nieger, E. Niecke and J. Tirree, Private Communication, 2002, CCD, 178050; (*b*) L. Heurer, D. Schromburg and R. Schmutzler, *Phosphorus, Sulfur Silicon Relat. Elem.*, 1989, **45**, 217.

21 (*a*) L. P. Ho, A. Nasr, P. G. Jones, A. Altun, F. Neese, G. Bistoni and M. Tamm, *Chem.–Eur. J.*, 2018, **24**, 18922; (*b*) Y.-y. Carpenter, N. Burford, M. D. Lumsden and R. McDonald, *Inorg. Chem.*, 2011, **50**, 3342.

22 S. Aime, R. K. Harris, E. M. McVicker and M. Fild, *J. Chem. Soc., Dalton Trans.*, 1976, 2144.

23 (*a*) V. Robert, S. Petit, S. A. Borshch and B. Bigot, *J. Phys. Chem. A*, 2000, **104**, 4586; (*b*) S. K. Latypov, F. M. Polyancev, D. G. Yakhvarov and O. G. Sinyashin, *Phys. Chem. Chem. Phys.*, 2015, **17**, 6976.

24 (*a*) D. A. Klumpp, *Chem.–Eur. J.*, 2008, **14**, 2004; (*b*) D. Schröder and H. Schwarz, *J. Phys. Chem. A*, 1999, **103**, 7385.

25 (*a*) G. A. Olah, G. Rasul, A. K. Yudin, A. Burrichter, G. K. S. Prakash, A. L. Chistyakov, I. V. Stankevich, I. S. Akhrem, N. P. Gambaryan and M. E. Vol'pin, *J. Am. Chem. Soc.*, 1996, **118**, 1446; (*b*) G. K. S. Prakash, T. Mathew, D. Hoole, P. M. Esteves, Q. Wang, G. Rasul and

G. A. Olah, *J. Am. Chem. Soc.*, 2004, **126**, 15770; (*c*) R. Weiss and S. Engel, *Angew. Chem., Int. Ed.*, 1992, **31**, 216; *Angew. Chem.*, 1992, **104**, 239; (*d*) F. G. Pühlhofer and R. Weiss, *Eur. J. Inorg. Chem.*, 2004, 1002.

26 B. D. Ellis, C. A. Dyker, A. Decken and C. L. B. Macdonald, *Chem. Commun.*, 2005, 1965.

27 For related P_7 compounds see: (*a*) M. Donath, M. Bodensteiner and J. J. Weigand, *Chem.–Eur. J.*, 2014, **20**, 17306; (*b*) J. J. Weigand, M. H. Holthausen and R. Fröhlich, *Angew. Chem., Int. Ed.*, 2009, **48**, 295; *Angew. Chem.*, 2009, **121**, 301; (*c*) W. Hönle, H. G. von Schnering, A. Schmidpeter and G. Burget, *Angew. Chem., Int. Ed. Engl.*, 1984, **23**, 817; *Angew. Chem.*, 1984, **96**, 796; (*d*) C. Mujica, D. Weber and H.-G. von Schnering, *Z. Naturforsch., B: J. Chem. Sci.*, 1986, **41b**, 991.

28 (*a*) S. Roy, S. K. S. Mazinani, T. L. Groy, L. Gan, P. Tarakeshwar, V. Mujica and A. K. Jones, *Inorg. Chem.*, 2014, **53**, 8919; (*b*) L. D. Field, R. W. Guest and P. Turner, *Inorg. Chem.*, 2010, **49**, 9086; (*c*) C. Federsel, A. Boddien, R. Jackstell, R. Jennerhahn, P. J. Dyson, R. Scopelliti, G. Laurenczy and M. Beller, *Angew. Chem., Int. Ed.*, 2010, **49**, 9777; *Angew. Chem.*, 2010, **122**, 9971.

29 J. F. Binder, S. C. Kosnik and C. L. B. Macdonald, *Chem.–Eur. J.*, 2018, **24**, 3556.

30 C. A. Tolman, *Chem. Rev.*, 1977, **77**, 313.

31 H. Mahnke, R. J. Clark, R. Rosanske and R. K. Sheline, *J. Chem. Phys.*, 1974, **60**, 2997.

32 (*a*) M. Alcarazo, *Chem.–Eur. J.*, 2014, **20**, 7968; (*b*) M. Alcarazo, *Acc. Chem. Res.*, 2016, **49**, 1797.

33 K. Schwedtmann, M. H. Holthausen, C. H. Sala, F. Hennersdorf, R. Fröhlich and J. J. Weigand, *Chem. Commun.*, 2016, **52**, 1409.

34 S. C. Kosnik, J. F. Binder, M. C. Nascimento, A. Swidan and C. L. B. Macdonald, *Chem.–Eur. J.*, 2019, **25**, 1208.

35 (*a*) J. Chatt, P. B. Hitchcock, A. Pidcock, C. P. Warrens and K. R. Dixon, *J. Chem. Soc., Dalton Trans.*, 1984, 2237; (*b*) J. Chatt, P. B. Hitchcock, A. Pidcock, C. P. Warrens and K. R. Dixon, *J. Chem. Soc., Dalton Trans.*, 1982, 932.

36 (*a*) O. Kühl, *Phosphorus-31 NMR Spectroscopy*, Springer, Heidelberg, 2008; (*b*) A. Pidcock, R. E. Richards and L. M. Venanzi, *J. Chem. Soc. A*, 1966, 1707.

37 I. G. Phillips, R. G. Ball and R. G. Cavell, *Inorg. Chem.*, 1992, **31**, 1633.

38 (*a*) S. Gómez-Ruiz and E. Hey-Hawkins, *Dalton Trans.*, 2007, 5678; (*b*) S. Gómez-Ruiz and E. Hey-Hawkins, *Coord. Chem. Rev.*, 2011, **255**, 1360.

39 (*a*) H. Kawai, W. J. Wolf, A. G. DiPasquale, M. S. Winston and F. D. Toste, *J. Am. Chem. Soc.*, 2016, **138**, 587; (*b*) O. Schuster and H. Schmidbaur, *Organometallics*, 2005, **24**, 2289; (*c*) O. Schuster, R.-Y. Liau, A. Schier and H. Schmidbaur, *Inorg. Chim. Acta*, 2005, **358**, 1429.